PET Imaging of Brain 5-HT_{1A} Receptors in Rat In Vivo with ^{18}F-FCWAY and Improvement by Successful Inhibition of Radioligand Defluorination with Miconazole

Dnyanesh N. Tipre, PhD[1]; Sami S. Zoghbi, PhD[1]; Jeih-San Liow, PhD[1]; Michael V. Green, MS[2]; Jurgen Seidel, PhD[3]; Masanori Ichise, MD[1]; Robert B. Innis, PhD[1]; and Victor W. Pike, PhD[1]

[1]Molecular Imaging Branch, National Institute of Mental Health, National Institutes of Health, Bethesda, Maryland; [2]Trident Imaging, Inc., Rockville, Maryland; and [3]Imaging Physics Laboratory, National Institute for Biomedical Imaging and Bioengineering, National Institutes of Health, Bethesda, Maryland

^{18}F-FCWAY (^{18}F-trans-4-fluoro-N-(2-[4-(2-methoxyphenyl) piperazin-1-yl)ethyl]-N-(2-pyridyl)cyclohexanecarboxamide) is useful in clinical research with PET for measuring serotonin 1A (5-HT_{1A}) receptor densities in brain regions of human subjects but has significant bone uptake of radioactivity due to defluorination. The uptake of radioactivity in skull compromises the accuracy of measurements of 5-HT_{1A} receptor densities in adjacent areas of brain because of spillover of radioactivity through the partial-volume effect. Our aim was to demonstrate with a rat model that defluorination of ^{18}F-FCWAY may be inhibited in vivo to improve its applicability to measuring brain regional 5-HT_{1A} receptor densities. **Methods:** PET of rat head after administration of ^{18}F-FCWAY was used to confirm that the distribution of radioactivity measured in brain is dominated by binding to 5-HT_{1A} receptors and to reveal the extent of defluorination of ^{18}F-FCWAY in vivo as represented by radioactivity (^{18}F-fluoride ion) uptake in skull. Cimetidine, diclofenac, and miconazole, known inhibitors of CYP450 2EI, were tested for the ability to inhibit defluorination of ^{18}F-FCWAY in rat liver microsomes in vitro. The effects of miconazole treatment of rats on skull radioactivity uptake and, in turn, its spillover on brain 5-HT_{1A} receptor imaging were assessed by PET with venous blood analysis. **Results:** PET confirmed the potential of ^{18}F-FCWAY to act as a radioligand for 5-HT_{1A} receptors in rat brain and also revealed extensive defluorination. In rat liver microsomes in vitro, defluorination of ^{18}F-FCWAY was almost completely inhibited by miconazole and, to a less extent, by diclofenac. In PET experiments, treatment of rats with miconazole nitrate (60 mg/kg intravenously) over the 45-min period before administration of ^{18}F-FCWAY almost obliterated defluorination and bone uptake of radioactivity. Also, brain radioactivity almost doubled while the ratio of radioactivity in receptor-rich ventral hippocampus to that in receptor-poor cerebellum almost tripled to 14. The plasma half-life of radioligand was also extended by miconazole treatment. **Conclusion:** Miconazole treatment, by eliminating defluorination of ^{18}F-FCWAY, results in effective imaging of brain 5-HT_{1A} receptors in rat. ^{18}F-FCWAY PET in miconazole-treated rats can serve as an effective platform for investigating 5-HT_{1A} receptors in rodent models of neuropsychiatric conditions or drug action.

Key Words: ^{18}F-FCWAY; miconazole; defluorination; 5-HT_{1A} receptors; rat; PET

J Nucl Med 2006; 47:345–353

PET is a noninvasive imaging technique that is useful for displaying and quantitatively measuring biological parameters in living subjects (*1–3*). For such purposes PET makes use of biologically relevant compounds labeled with positron-emitting nuclides (i.e., radiotracers/radioligands) (*1,4–6*). PET now plays an important role in the investigation of neuropsychiatric disorders because, when coupled with suitably effective radioligands (*5*), it allows measurement of the density of important biological markers (e.g., enzymes, receptors, and transporters) (*7,8*). Moreover, PET may be used to determine the occupancy of such targets by established therapeutics or developmental drugs (*8–10*). The sensitivity and accuracy of PET measurements of the binding potential of neuroreceptors in brain may be adversely affected by metabolism of the used radioligand, especially if the radioactive metabolites enter brain or appear in regions close to brain regions subject to measurement. In some cases, ^{18}F-labeled PET ligands undergo rapid defluorination in vivo to ^{18}F-fluoride ion which is then taken up into bone, including skull. This is the case in human subjects for ^{18}F-FCWAY (^{18}F-trans-4-fluoro-N-(2-[4-(2-methoxyphenyl) piperazin-1-yl)ethyl]-N-(2-pyridyl)cyclohexanecarboxamide, **1**) (*11*), a valuable radioligand for measuring 5-HT_{1A} receptors in human brain with PET. This radioligand has already been applied in clinical research on, for example, panic disorders (*12*) and epilepsy (*13*). However, skull uptake of radioactivity is significant and may represent twice the whole brain average at 60 min after radioligand injection (*14*).

Received Jul. 24, 2005; revision accepted Nov. 7, 2005.

For correspondence or reprints contact: Dnyanesh N. Tipre, PhD, National Institutes of Health, Bldg. 1, Room B3-10, 1 Center Dr., MSC 0135, Bethesda, MD 20892-0135.

E-mail: dnyanesht@yahoo.com

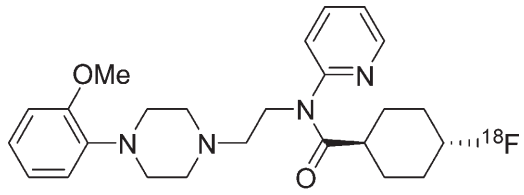

1, [^{18}F]FCWAY

In clinical research with PET, it is sometimes desirable to measure serotonin 1A (5-HT_{1A}) receptor densities close to the skull, besides structures deeper in the brain. The accumulation of radioactivity in skull exacerbates these measurements through a partial-volume effect in which radioactivity in skull is detected as radioactivity in brain and vice versa and also through the greater difficulty of physically defining regions of interest (ROIs) for biomathematic analysis. The partial-volume effect arises from the limited resolution of PET cameras (at best, a few millimeters) and the uncertainty of the locations of positron annihilation events in relation to the corresponding locations of positron emission (also of the order of millimeters separation in tissue). The definition of ROIs may be assisted by coregistration with MRI scans of the head. Hence, a means to block the defluorination of ^{18}F-FCWAY in vivo should avoid the undesirable effects of skull radioactivity when making 5-HT_{1A} receptor measurements in the ROIs close to skull and would further increase the value of this radioligand for biological and clinical research.

Defluorination of certain aliphatic compounds is known to be a phase I reaction occurring primarily through the action of cytochrome P450 2E1 (CYP2E1) isozyme in liver microsomes (*15,16*). We postulated that this isozyme, or related enzymes, might be responsible for the defluorination of ^{18}F-FCWAY and that known CYP2E1 inhibitors might usefully suppress the defluorination of ^{18}F-FCWAY in vivo and thereby reduce the impact of the partial-volume effect (spillover).

The aims of this study were to (i) assess the efficacy of ^{18}F-FCWAY with PET for imaging 5-HT_{1A} receptors in rat brain, (ii) measure the degree of defluorination of ^{18}F-FCWAY and the skull uptake of ^{18}F-fluoride ion in rat in vivo, (iii) inhibit defluorination of ^{18}F-FCWAY in rat in vivo, and (iv) assess the effect of inhibition of defluorination of ^{18}F-FCWAY on PET image quality.

MATERIALS AND METHODS

Chemicals, including cimetidine, diclofenac, and miconazole nitrate, and high-performance liquid chromatography (HPLC)–grade solvents were purchased from Sigma Aldrich Chemical Co.. Rat liver microsomes were obtained from Invitrogen and stored at 70°C before use. ^{18}F-Fluoride ion was produced with the cyclotron-induced ^{18}O(p,n)^{18}F reaction on ^{18}O-enriched water and dissolved in sodium phosphate buffer (0.1 mol/L; pH 7.4). ^{18}F-FCWAY was prepared from cyclotron-produced ^{18}F-fluoride ion, as reported (*11*). The average radiochemical purity and specific radioactivity of ^{18}F-FCWAY at the end of radiosynthesis were 99.5% and 48.1 GBq/μmol (range, 40.6–55.3 GBq/μmol), respectively. Radioactivity was measured in a calibrated ionization chamber (Capintec Inc.) or an automatic well-type γ-counter (Wallac Wizard 3″; Perkin Elmer). All radioactive samples counted in the γ-counter were controlled by allowing decay to levels that neither cause count loss due to dead time nor counting errors exceeding 1.0% at 2 SD. Each radiotracer (^{18}F-fluoride ion or ^{18}F-FCWAY) was used within 20 min of its radiosynthesis. In vitro incubations were performed in borosilicate test tubes (VWR International) at 37°C. Thin-layer chromatography (TLC) was performed on silica gel layers (SIL G, UV/254; Alltech Associates Inc.). Samples (<1.8–3.7 MBq) were spotted on the layers and dried at room temperature (RT). Layers were then developed to a height of at least 10 cm with methanol/chloroform/glacial acetic acid (1:1:0.5 v/v/v) and then read with a radio-TLC scanner (model AR-2000; Bioscan). The separation of ^{18}F-fluoride ion (R_f = 0) from radiometabolites (R_f = 0.6–0.8) and ^{18}F-FCWAY (R_f = 0.85) was confirmed by comigration with added authentic ^{18}F-fluoride ion and ^{18}F-FCWAY.

Investigation of Defluorination of ^{18}F-FCWAY In Vitro

Stock solutions of magnesium chloride (0.1 mol/L) and β-nicotinamide adenine dinucleotide phosphate (reduced NADPH; 8 mmol/L) and a stock suspension of rat liver microsomes (20 mg/mL) were each prepared in buffer (sodium phosphate, 0.1 mol/L; pH 7.4). ^{18}F-FCWAY (3.7 MBq) in buffer (10 μL) was mixed with (i) buffer (490 μL), (ii) rat whole blood (490 μL), (iii) rat liver microsomal suspension (25 μL) plus magnesium chloride solution (25 μL) in buffer (440 μL), or (iv) rat liver microsomal suspension (25 μL), magnesium chloride solution (25 μL), plus NADPH solution (62 μL) in buffer (378 μL). The mixtures were incubated separately at 37°C for 30 min. An aliquot (50 μL) was then removed and mixed with an equal volume of ice-cold acetonitrile and centrifuged. The supernatant liquid was analyzed with radio-TLC.

Effect of Alcohol on Liver Microsomal Enzyme Activity

The experiment described above with rat liver microsomes in the presence of NADPH was repeated with ethanol in the incubation mixture at final concentrations of 0.05%, 0.5%, 1.0%, or 5.0% (v/v).

Effect of CYP2E1 Inhibitors on Defluorination of ^{18}F-FCWAY in Rat Liver Microsomes

Stock solutions of magnesium chloride and NADPH and a suspension of rat liver microsomes in buffer were prepared as described above. Stock solutions of cimetidine (1 mmol/L), diclofenac sodium (10 mmol/L), and miconazole nitrate (0.3 mmol/L) were each prepared in aqueous ethanol (10% v/v). ^{18}F-FCWAY (3.7 MBq) in buffer (10 μL) was mixed with rat liver microsomal suspension (25 μL) and magnesium chloride solution (25 μL) in buffer (378 μL) in 3 separate test tubes. Stock solution of a different inhibitor (25 μL) was added to each tube and reactions were initiated by adding NADPH solution (62 μL) to each tube. Mixtures were incubated at 37°C for 30 min. An aliquot of each mixture (50 μL) was then removed and mixed with an equal volume of ice-cold acetonitrile and centrifuged. The supernatant liquid was analyzed with radio-TLC. A control experiment was performed without inhibitor.

Animal Preparation for PET

All animal procedures were performed in strict accordance with the National Institutes of Health (NIH) Guide for Care and Use of Laboratory Animals and approved by the National Institute of Mental Health (NIMH) Animal Care and Use Committee. Male Sprague–Dawley rats (250–350 g) were used for PET in vivo. The rats were housed in pairs and allowed food and water ad libitum. For in vivo experiments, each rat was anesthetized with 1.5% isoflurane in oxygen and kept in prone position on the scanner bed with head centered in the gantry of the PET camera. For PET experiments without blood sampling, inhibitor and radioligand were administered to the anesthetized rat via a single catheter in the penile vein. For PET experiments with blood sampling, inhibitor and radioligand were given via a single catheter in the tail vein and blood was sampled via a catheter from the penile vein. The catheters (30- to 35-cm polyethylene; PE 10; dead space, 0.05–0.07 mL; Intramedic; Clay Adams) were secured with tissue adhesive (3 M Vetbond; 3M Animal Care Products). Throughout the scanning procedure, body temperature in the anesthetized rat was monitored by a rectal temperature probe and maintained between 36.5°C and 37.5°C by a heating lamp and heating pad.

PET

Paired rats were used in control and all other experimental treatments. Imaging was performed with the NIH Advanced Technology Laboratory Animal Scanner (ATLAS) (*17*) with an effective transaxial field of view of 6.4 cm and an axial field of view of 2.0 cm. The reconstructed voxel size was $0.56 \times 0.56 \times 1.11$ mm. Coronal section images were created for subsequent data analysis. PET images were reconstructed by a 3-dimensional ordered-subset expectation maximization (OSEM) algorithm (3 iterations and 16 subsets), achieving 1.6-mm full width at half maximum resolution at the center (*18,19*). Image data were not corrected for attenuation or scatter. Tomographic images were analyzed with PMOD 2.5 (pixelwise modeling computer software; PMOD Group). After identification of the various rat brain structures on PET images with MRI coregistration, ROIs associated with frontal cortex, frontal hippocampus, ventral hippocampus, and cerebellum were drawn on all rat brain coronal images, guided by stereotactic coordinates (*20*). The decay-corrected time–activity curves were presented in units of percentage of the standardized uptake value (SUV), calculated as (% injected dose/cm^3) × body weight (g) to normalize for the differences in rat weight and administered dose and to allow comparison of inter-rat and inter-organ data. All percentage SUV values in the text are the mean of measurements in 2 rats. Cerebellar radioactivity concentrations were subtracted from those in each of the reported brain regions to give regional specific binding concentrations in percentage SUV.

Brain and Skull Radioactivity Uptake Measured with PET: Comparison with Ex Vivo Measurement

Rats were injected intravenously with either ^{18}F-FCWAY (33.3–48.1 MBq) or ^{18}F-fluoride ion (37–44.4 MBq) in sodium phosphate buffer (0.1 mol/L; pH 7.4) via the penile vein. For each rat, the dynamic emission scan was recorded for 90 min and the rat was euthanized under anesthesia with an intravenous injection of 2 mEq of potassium chloride (American Pharmaceutical Partners, Inc.) in a 1-mL volume. The brain and upper section of skull were dissected and weighed, and the radioactivity contents were measured in a γ-counter. Ex vivo brain and upper skull radioactivities were compared with the in vivo radioactivities measured on PET images at 90 min.

Inhibition of ^{18}F-FCWAY Metabolism In Vivo Measured with PET: Comparison with Ex Vivo Measurement

Isotonic aqueous miconazole nitrate for intravenous infusion was prepared in a vehicle composed of Captisol (sulfobutyl ether β-cyclodextrin (sodium); 75 mmol/L; Cydex Inc) and lactic acid (50 mmol/L), as described previously (*21*). Pairs of rats were pretreated with miconazole nitrate (15, 30, or 60 mg/kg intravenously) via the penile vein at an infusion rate of 22 μL/min for 45 min. ^{18}F-FCWAY (33.3–48.1 MBq) was promptly injected over 15 s via the penile vein and dynamic PET emission scans were recorded for 90 min. Control rats were injected with ^{18}F-FCWAY alone with no other treatment. Any effect of the vehicle (Captisol) on imaging with ^{18}F-FCWAY was determined in a pair of rats by administering ^{18}F-FCWAY and the vehicle at the same concentration as in other experiments where the effect of miconazole nitrate was studied. At the end of each scan, the rats were euthanized under anesthesia by intravenous injection of potassium chloride (2 mEq; 1 mL). The brain and upper section of skull were dissected, removed, and weighed, and the radioactivity contents were measured and compared with the radioactivities on PET images, as described.

Determination of Radioactive Metabolites of ^{18}F-FCWAY in Rat Plasma by HPLC

^{18}F-FCWAY (37–44.4 MBq) was injected into the rat via the tail vein. Blood samples (250 μL) were collected via the penile vein into heparinized tubes at different times (3, 7, 10, 15, 20, 30, 40, 60, 80, and 90 min) after radioligand injection and centrifuged at 1,800*g* for 1.5 min at RT to separate plasma. Each plasma sample (50–100 μL) was then transferred to a test tube containing acetonitrile (700 μL) and mixed well. Water (100 μL) was added with thorough mixing. Each tube was counted in the γ-counter for total plasma radioactivity and centrifuged at 9,400*g* for 2 min. In these experiments, no attempt was made to enhance the efficiency of ^{18}F-fluoride ion extraction by adding carrier fluoride ion preceding extractions. The supernatant liquid was injected onto the radio-HPLC column. Each precipitate was measured in the γ-counter to allow monitoring of and correction for the percentage recovery of radioactivity in the supernatant liquids. Radio-HPLC was performed on a Novapak C_{18} column (100 × 8.0 mm; Waters Corp.) with a radial compression module RCM-100, eluted with methanol/water/triethylamine (80:20:0.1 v/v/v) at 1.5 mL/min. Eluate was monitored with an in-line flow-through Na(Tl) scintillation detector (Bioscan). Chromatographic data were corrected for physical decay (^{18}F, half-life = 109.77 min), stored, and analyzed by Bio-Chrom Lite software (Bioscan). All plasma radioactivity measurements were further corrected for their radiocomposition using radio-HPLC results and then were decay corrected to the time of dose administration. Unextracted quantities of radioactivity were considered in the calculation of the final parent radioligand concentration in plasma at each sampling time. The experiment was repeated, with each rat pretreated by infusion (22 μL/min) with miconazole nitrate (30 mg/kg intravenously) via the tail vein for 45 min. Areas under the curve between zero and infinity were calculated for each rat after monoexponential curve fitting of the plasma concentration of parent radioligand (% SUV).

RESULTS

Inhibition of ^{18}F-FCWAY Defluorination: In Vitro

^{18}F-Fluoride ion (R_f = 0), radiometabolites of ^{18}F-FCWAY (R_f = 0.55–0.80) and ^{18}F-FCWAY (R_f = 0.85) were well resolved with radio-TLC on silica gel layers. Defluorination of ^{18}F-FCWAY was not observed in phosphate buffer (pH 7.4) or rat whole blood. Metabolism of radioligand leading to defluorination (13% in 30 min) was observed in rat liver microsomes only in the presence of NADPH.

When ^{18}F-FCWAY was incubated with rat liver microsomes, NADPH, and various concentrations of ethanol (0%, 0.05%, 0.50%, 1.00%, or 5.00% v/v) for 30 min, defluorination of the radioligand was 13%, 13%, 13%, 9%, or 4%, respectively. When ^{18}F-FCWAY was incubated with rat liver microsomes and NADPH in aqueous ethanol (≤0.5% v/v) for 30 min, defluorination in the presence of cimetidine (50 μmol/L), diclofenac (500 μmol/L), miconazole (15 μmol/L), or control (without inhibitor) was 13%, 5%, 2%, or 13%, respectively.

PET in Rat with ^{18}F-FCWAY (No Treatment)

After injection of ^{18}F-FCWAY into rat, image analysis revealed moderately high uptake of radioactivity into whole brain and 5-HT_{1A} receptor-rich regions (frontal cortex, frontal hippocampus, and ventral hippocampus) over the early phase of the scan (~15 min) followed by a slow clearance of radioactivity (Fig. 1A). In 5-HT_{1A} receptor-poor cerebellum the early uptake of radioactivity was similar to that in other regions, but radioactivity concentration rapidly declined to a low and an apparently stable level of about 50% SUV. The PET ratios of radioactivity in frontal cortex, frontal hippocampus, and ventral hippocampus to that in cerebellum reached 4.6, 5.5, and 4.8 at 15 min after injection, respectively, and then slowly declined (Fig. 2A).

PET images acquired between 50 and 60 min after radioligand injection showed a brain distribution of radioactivity that was consistent with primarily specific binding of radioligand to 5-HT_{1A} receptors (Fig. 3B). However, PET images were dominated by high radioactivity in skull. Skull radioactivity increased continuously soon after radioligand injection and, according to PET, reached 630% SUV at 90 min (Fig. 4), a value substantially higher than recorded in brain (137% SUV). The corresponding ex vivo measures of skull (Fig. 5A) and brain (Fig. 5B) radioactivities were 500% and 41% SUV, respectively.

PET images obtained from rats that were injected with ^{18}F-FCWAY and the vehicle Captisol reproduced those obtained from the rat injected with ^{18}F-FCWAY alone.

PET in Rat with ^{18}F-Fluoride Ion

Injection of ^{18}F-fluoride ion alone into rat for PET with ATLAS resulted in a rapid high initial uptake of radioactivity into skull, which thereafter gradually increased with apparently parallel but lower uptakes of radioactivity in ventral hippocampus and whole brain (Fig. 6). Apparent uptake was higher in ventral hippocampus (near the skull) than that in whole brain, as strikingly visible in the PET image of the rat head (Fig. 3A). Ex vivo measurements of radioactivity at 90 min after the injection of ^{18}F-fluoride ion into the rat showed that the SUV in brain was 5%, whereas the PET camera recorded 60% SUV.

Inhibition of ^{18}F-FCWAY Defluorination: In Vivo

Before intravenous administration of ^{18}F-FCWAY, rats were pretreated with 0, 15, 30, or 60 mg/kg miconazole nitrate. PET indicated that the skull uptake of radioactivity

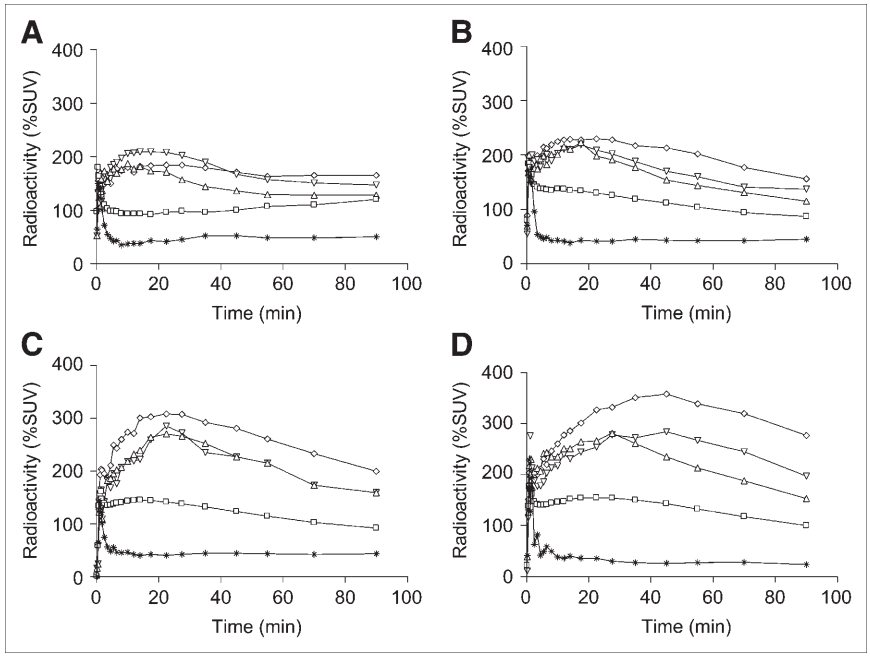

FIGURE 1. Time–activity curves in frontal cortex (△), frontal hippocampus (▽), ventral hippocampus (◇), cerebellum (*), and brain (□) in rats infused intravenously for 45 min with 0 (A), 15 (B), 30 (C), or 60 (D) mg/kg of miconazole nitrate immediately before being injected intravenously with ^{18}F-FCWAY (33.3–48.1 MBq). Each panel shows data from 1 rat.

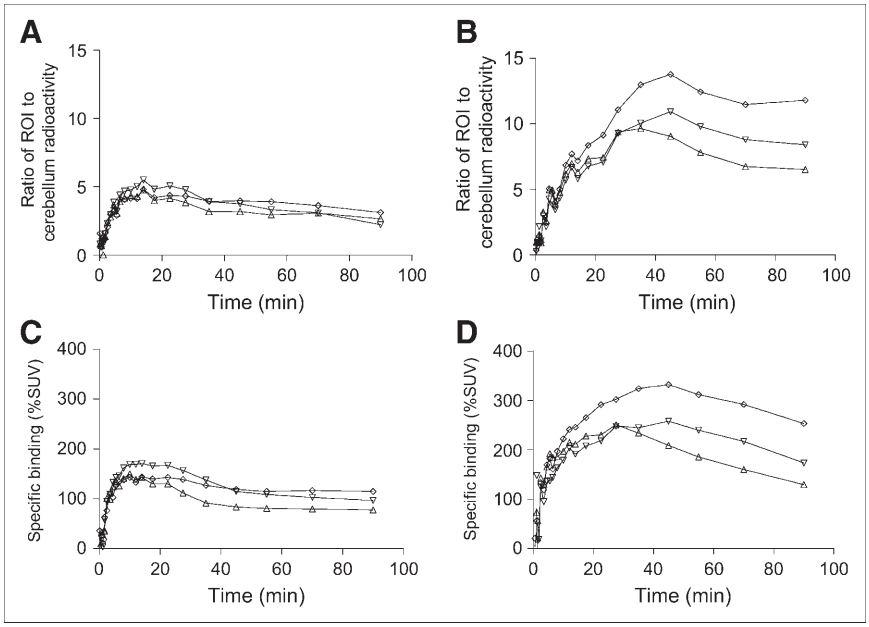

FIGURE 2. Ratios of radioactivity in the ROIs frontal cortex (△), frontal hippocampus (▽), and ventral hippocampus (◇) to that in cerebellum after intravenous injection of ^{18}F-FCWAY into rats under baseline conditions (A) or in rats treated with 60 mg/kg miconazole nitrate (B). C and D show, for the experiments presented in A and B, respectively, the level of 5-HT_{1A} receptor-specific binding in frontal cortex (△), frontal hippocampus (▽), and ventral hippocampus (◇), expressed in percentage SUV of the difference in radioactivity concentration between brain tissue of interest and cerebellum Each panel shows data from 1 rat.

was gradual in each experiment (Fig. 4) and at 90 min after radioligand administration it was 630%, 300%, 180%, and 82% SUV, respectively (Fig. 5A). The corresponding ex vivo measures were 500%, 250%, 127%, and 59% SUV (Fig. 5A). The ratios of in vivo measurements taken by ATLAS to those ex vivo skull radioactivities measured in the γ-counter are 1.26, 1.20, 1.35, and 1.39, respectively.

In the same experiments, for treatment with 0, 15, 30, and 60 mg/kg miconazole nitrate, brain radioactivity at 90 min measured by PET was 137%, 75%, 68%, and 89% SUV, whereas brain radioactivities measured ex vivo were 41%, 47%, 52%, and 74% SUV, respectively (Fig. 5B). The ratios of in vivo to ex vivo brain radioactivities are 3.34, 1.60, 1.31, and 1.20, respectively.

Reduced spillover of radioactivity from skull to brain in PET measurements, coupled with increasing brain uptake of radioligand with escalating miconazole dose, were observable in acquired PET images of brain (Figs. 3B–3E) and in the time–activity curves for brain (Figs. 1A–1D). The corresponding PET time–activity curves for 5-HT_{1A} receptor regions (frontal cortex, frontal hippocampus, and ventral hippocampus) also showed increased uptake of radioactivity as miconazole dose was increased, with maximal radioactivity uptake also delayed to later times after injection (Figs. 1A–1D). For the PET experiment in which the highest dose of miconazole was given, the maximal ratios of radioactivity in frontal cortex, frontal hippocampus,

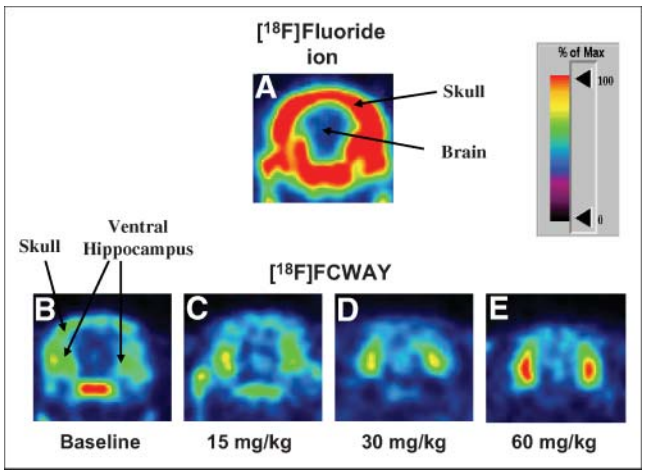

FIGURE 3. PET scans of the head acquired between 50 and 60 min after intravenous injection of rat with ^{18}F-fluoride ion (A), ^{18}F-FCWAY (B), miconazole nitrate (15 mg/kg intravenously) and then ^{18}F-FCWAY (C), miconazole nitrate (30 mg/kg intravenously) and then ^{18}F-FCWAY (D), and miconazole nitrate (60 mg/kg intravenously) and then ^{18}F-FCWAY (E). % of Max = percentage of maximum.

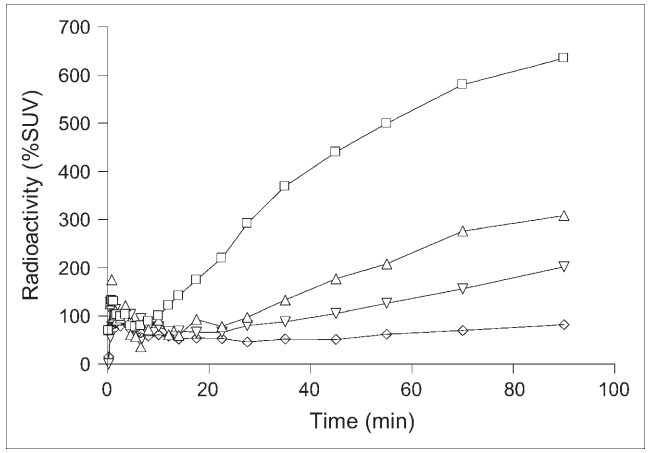

FIGURE 4. Time–activity curves in skull in rats treated with 0 (□), 15 (△), 30 (▽), or 60 (◇) mg/kg of miconazole nitrate immediately before intravenous injection of ^{18}F-FCWAY. Each panel shows data from 1 rat.

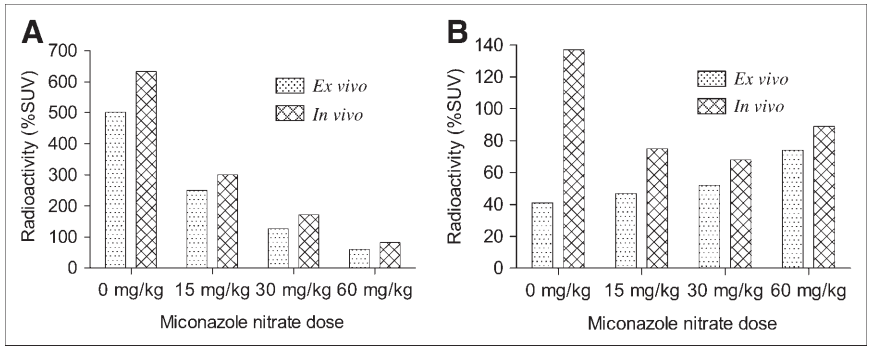

FIGURE 5. Skull (A) and brain (B) radioactivities (% SUV) measured in vivo with PET and ex vivo at 90 min after ^{18}F-FCWAY injection in rats treated with 0, 15, 30, and 60 mg/kg miconazole nitrate.

and ventral hippocampus to that in cerebellum were 9.6 at 35 min, 10.9 at 45 min, and 13.8 at 45 min, respectively (Fig. 2B). In the same experiment, the specific binding values (% SUV) of radioactivity in frontal cortex, frontal hippocampus, and ventral hippocampus reached 251 at 27 min, 248 at 27 min, and 332 at 45 min, respectively (Fig. 2D). These values are about 2- to 3-fold higher than those in the control experiment (Fig. 2C).

Throughout the PET experiment with the highest dose of miconazole nitrate, the radioactivity in cerebellum (Fig. 1D) appeared generally lower than that in the control experiment (Fig. 1A). In experiments with intermediate doses the cerebellum radioactivity is not generally reduced but is generally similar to control over the time courses of the experiment (Figs. 1B and 1C).

HPLC Analysis of Rat Plasma After ^{18}F-FCWAY Administration

After intravenous injection of ^{18}F-FCWAY into rat, plasma samples were deproteinized by addition of acetonitrile and analyzed by reverse-phase HPLC. The recovery of radioactivity from control rat plasma was 95% for a sample taken at 3 min after injection and thereafter declined gradually with sampling time (to 50% at 90 min after injection), whereas the extraction of radioactivity from plasma from the miconazole-treated rats was averaged 88% throughout the sampling period. HPLC analysis of plasma samples obtained from the miconazole-treated rats showed 3 radioactive peaks. The most polar radioactive peak eluted with the void volume. This was followed closely by the second peak and, finally, the well-separated peak of parent radioligand. Radiochromatograms from control rat plasma showed 2 radioactive peaks, one broad peak associated with the void volume, possibly composed of 2 or more unresolved peaks, and a later well-resolved peak for parent radioligand. The recoveries of radioactivities from the HPLC column were quantitative as monitored by both recovery of known amounts of injected plasma radioactivities and by injection of absolute methanol (2 mL) and absence of radioactivity elution.

Reverse-phase HPLC analysis of the plasma of 1 rat administered miconazole nitrate (30 mg/kg) before injection of ^{18}F-FCWAY and of a control rat administered radioligand alone, showed that the plasma half-lives of radioligand were 19.5 and 11.2 min and that the corresponding areas under the curve between 0 min and infinity were 1,420% and 940% SUV × min, respectively.

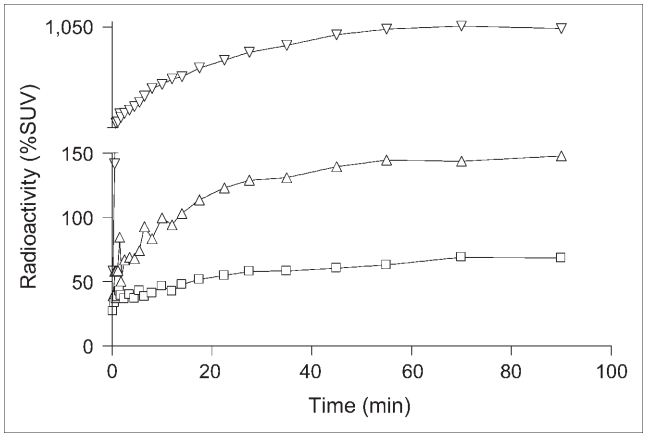

FIGURE 6. Time–activity curves in ventral hippocampus (△), brain (□), and skull (▽) after intravenous injection of ^{18}F-fluoride ion into rats. Each panel shows data from 1 rat.

DISCUSSION

Inhibition of ^{18}F-FCWAY Defluorination: In Vitro

The possibility to inhibit ^{18}F-FCWAY defluorination was first explored in vitro. ^{18}F-Fluoride ion, radiometabolites of ^{18}F-FCWAY, and ^{18}F-FCWAY were well resolved by TLC on silica gel layers. Hence, radio-TLC was used to quantify ^{18}F-FCWAY defluorination in experiments performed in vitro. ^{18}F-FCWAY was found to be chemically stable at physiological pH (7.4) and in whole blood. Metabolism of ^{18}F-FCWAY leading to defluorination was observed in rat liver microsomes only in the presence of NADPH, thus indicating the possible involvement of cytochrome P450 enzymes in defluorination (*22*).

Because the defluorination of some aliphatic compounds is known to be a phase I reaction occurring primarily through the actions of CYP2E1 isozyme (*15*), known CYP2E1 inhibitors were screened for their potency to inhibit defluorination of ^{18}F-FCWAY in rat liver microsomes in vitro. Cimetidine (inhibitor of CYP1A2, CYP2C9, CYP2C19, CYP2D6, CYP2E1, and CYP11B1) (*23,24*), diclofenac (inhibitor of CYP2C9 and CYP2E1) (*25,26*), and miconazole (a potent inhibitor of CYP2E1 (*26*) and a less potent

inhibitor of CYP3A4 and CYP11B1) (*27,28*) were investigated at 50, 500, and 15 μmol/L concentration, respectively. The concentration of cimetidine used in this experiment was determined by its upper limit of solubility in 0.5% (v/v) ethanol. The concentrations of diclofenac and miconazole were selected by consideration of the reported inhibition constants (K_i) of these drugs (500 and 15 μmol/L) for CYP2E1 isozyme (*24,26,29*).

The enzyme inhibitors were dissolved in aqueous ethanol and, therefore, the effect of ethanol on the viability of CYP enzymes was questionable. At a concentration up to 0.5% (v/v), ethanol was found to have no detectable effect on the defluorination ability of microsomal CYP enzymes. Therefore, 0.5% aqueous ethanol was considered to be a suitable medium for exploring the metabolism of ^{18}F-FCWAY in vitro. Defluorination of ^{18}F-FCWAY in the presence of miconazole (15 μmol/L) was substantially lower than that in the presence of cimetidine (50 μmol/L) or diclofenac (500 μmol/L). In the literature there is no evidence that miconazole itself may cross the blood–brain barrier and no evidence that it may directly or indirectly affect brain 5-HT_{1A} density. Also, miconazole has been used for compassionate relief of meningitis in humans but only after intrathecal administration because it is considered to have low central nervous system penetration (*30,31*). In view of these favorable properties, miconazole was selected for further investigation of its ability to inhibit defluorination of ^{18}F-FCWAY in vivo.

PET in Rat with ^{18}F-FCWAY (No Treatment)

To test the efficacy of miconazole for inhibiting defluorination of ^{18}F-FCWAY in vivo and, consequently, for reducing skull radioactivity uptake, we wished to test the relevance of a model based on PET in the rat. We considered that a rat PET model would permit great flexibility in selecting inhibitor dose regimens and also provide for a high throughput of experiments with full kinetic data from key ROIs selected from the head (i.e., skull, cerebellum, ventral hippocampus, frontal hippocampus, and frontal cortex). The small-animal PET camera available to us for this study was the ATLAS camera, which has a resolution of 1.6 mm (*17*). This resolution is adequate for demarcation of the key ROIs, though partial-volume effects would be expected to be significant throughout the head. HPLC measurements of radioactive metabolites in plasma from rats that had been administered ^{18}F-FCWAY intravenously confirmed that appreciable defluorination of this radioligand occurs in this species (*11*) as it does in humans (*14*), though not in rhesus monkey (*32*).

^{18}F-FCWAY is well established as a radioligand for imaging 5-HT_{1A} receptors in large species (monkey and human) (*14,32*). Although some ex vivo findings have suggested that ^{18}F-FCWAY might be an effective radioligand in rat in vivo (*11*), to our knowledge, PET with ^{18}F-FCWAY in any small animal has not been reported previously. To make use of a rat-PET model, it was first essential to verify that ^{18}F-FCWAY was capable of revealing the distribution of 5-HT_{1A} receptors in rat brain with the ATLAS camera.

^{18}F-FCWAY was injected into rats at small doses (33.3–44.4 GBq/μmol) calculated to occupy <0.2% of brain receptors and, therefore, to have a negligible effect on receptor availability for imaging (*33,34*). PET revealed time–activity curves (Fig. 1A) that were consistent with mostly specific binding of radioligand to 5-HT_{1A} receptors. Ratios of radioactivity in frontal cortex, frontal hippocampus, and ventral hippocampus to that in cerebellum reached about 5 (Fig. 2A). Hence, there appeared to be a high proportion of ^{18}F-FCWAY bound specifically to 5-HT_{1A} receptors in these regions (Fig. 2C). However, PET images were dominated by high radioactivity in skull, attributed to ^{18}F-fluoride ion arising from extensive defluorination of the radioligand (Fig. 3B). The uptake of radioactivity in skull continuously increased soon after injection of radioligand and, according to PET measurement, reached as high as 550% SUV at 90 min (Fig. 4), a value substantially higher than that seen in brain (Fig. 1A).

PET in Rat with ^{18}F-Fluoride Ion

The thinness of the rat skull is comparable to the resolution of the ATLAS camera. Hence, any ROI drawn over skull or adjacent brain tissue will be subject to partial-volume effects causing spillover of radioactivity from skull to adjacent brain and vice versa. For PET with ^{18}F-FCWAY, this spillover will be most significant from the higher radioactivity levels in skull to the lower radioactivity levels in nearby areas of brain.

Spillover of radioactivity from skull to brain was verified by injecting ^{18}F-fluoride ion alone into rat for PET with ATLAS. This resulted in a rapid high initial uptake of radioactivity into skull, which gradually increased thereafter, with an apparently parallel but lower uptake of radioactivity in ventral hippocampus and whole brain (Fig. 6). Notably, apparent uptake was higher in ventral hippocampus (proximal to skull) than that in whole brain.

Our ex vivo measurements of radioactivity were devoid of significant dead-time or partial-volume effects and were in the range of instrument quantification with low counting error. They are therefore considered to be accurate. Ex vivo measurements of radioactivity at 90 min after injection of ^{18}F-fluoride ion into a rat showed that the SUV in brain was 5%, whereas the PET camera recorded 60% SUV, thereby confirming the sizeable impact of spillover on PET measurements. These ex vivo measurements confirmed the negligible ability of ^{18}F-fluoride ion to enter brain. They also indicated the potentially high magnitude of spillover of radioactivity from skull to brain in PET of ^{18}F-FCWAY in rat as a direct result of the appearance of ^{18}F-fluoride ion as a metabolite.

Inhibition of ^{18}F-FCWAY Defluorination: In Vivo

Subsequent comparison of PET and ex vivo measurements for a rat intravenously administered ^{18}F-FCWAY confirmed the very substantial spillover of radioactivity

from skull (^{18}F-fluoride ion metabolite) to brain (Fig. 5). In view of the ability of miconazole to inhibit defluorination of ^{18}F-FCWAY in vitro, the demonstrated efficacy of PET with ^{18}F-FCWAY to reveal 5-HT_{1A} receptors in rat brain, and the spillover of radioactivity from skull to brain in PET, we set out to test the ability of miconazole to inhibit the defluorination of ^{18}F-FCWAY in rat in vivo.

PET (Figs. 3B–3E and 4) and ex vivo measurements (Fig. 5A) consistently demonstrated that escalating doses of miconazole nitrate (up to 60 mg/kg) progressively reduced radioactivity uptake into skull after ^{18}F-FCWAY administration. Miconazole nitrate, at the highest tested dose (60 mg/kg intravenously), dramatically reduced the radioactivity concentration in skull by 87% (Fig. 4).

At 90 min after radioligand injection in control and miconazole-treated rats, the ratios of in vivo measurements in skull taken by ATLAS to those taken ex vivo in a γ-counter are quite similar (1.20–1.39) across a wide range of skull SUV values (Fig. 5A), indicating systematic error in either or both measurements. However, the sources of these errors were not identified. In the same experiment, with increasing miconazole nitrate dose, PET measurements indicate that brain radioactivity first decreases and finally increases, whereas ex vivo measures show a steady increase in brain radioactivity (Fig. 5B). Thus, the ratio of in vivo to ex vivo brain measures is high when radioactivity in skull is high. With decreasing radioactivity in skull, the ratio for brain decreases to about the ratio seen for skull. These findings are consistent with decreasing spillover of radioactivity from skull to brain in the PET measurements, coupled with increasing brain uptake of radioligand as miconazole dose is increased.

Treatment with miconazole not only decreased the spillover effect but also improved radioactivity uptake in 5-HT_{1A} receptor-rich regions (Figs. 1B–1D), ratios of radioactivity in these regions to that in cerebellum (Fig. 2B) and specific binding (Fig. 2D). After miconazole treatment, PET images had better contrast and reduced uptake of radioactivity in skull (Figs. 3B–3E). At the highest dose of miconazole treatment, the ratio of radioactivity in ventral hippocampus to that in cerebellum was almost tripled to 14, whereas the PET images were free of appreciable uptake of radioactivity in skull.

The great improvement in image contrast after miconazole treatment may be attributed to a combination of possible effects. One explanation is reduced spillover of radioactivity into brain, including cerebellum, which may reduce the denominator in ROI-to-cerebellum radioactivity ratios. This factor appears to be operating in the experiment with the highest dose of miconazole relative to the control experiment (Fig. 1D). However, throughout experiments with intermediate doses, the cerebellum radioactivity is not generally reduced but is similar to that in the control experiment (Figs. 1B and 1C). A second explanation is that inhibition of defluorination of ^{18}F-FCWAY results in increased availability of the radioligand for entry into brain. HPLC measurements of the time course of parent radioligand in the plasma of a control rat and a rat administered miconazole nitrate (30 mg/kg) before injection of ^{18}F-FCWAY supports the operation of this effect. For the miconazole-treated rat compared with the control, the plasma half-life of radioligand was prolonged by 74% and the areas under the curve increased by 51%.

Although the HPLC method used here was optimized to separate and quantify ^{18}F-FCWAY and not to identify radioactive metabolites, characteristic differences in the radiochromatographic behavior of plasma samples obtained from control and miconazole-treated rats were noted. The extraction of radioactivity from control rat plasma was less efficient than that from the plasma of the miconazole-treated rat, presumably because of the higher proportion of radioactivity represented by poorly extractable ^{18}F-fluoride ion. Moreover, the polar radioactive peak eluting near the void volume was broad and strong in the analysis of plasma samples from control rats and sharper and weaker in samples from miconazole-treated rats. These observations appear consistent with less metabolism of radioligand to ^{18}F-fluoride ion in the miconazole-treated rats.

Miconazole is efficient in reducing the in vivo defluorination of ^{18}F-FCWAY in rats, but because its oral or intravenous administration in human subjects is not approved in the United States, other pharmaceuticals that are equally effective in modulating the defluorination enzymes in humans will need to be identified before applying this approach to human studies.

CONCLUSION

This study has shown that (i) ^{18}F-FCWAY is subject to defluorination in liver microsomes in vitro and in rat in vivo, (ii) such defluorination greatly impairs brain 5-HT_{1A} receptor imaging with ^{18}F-FCWAY and PET in rat, due to spillover of radioactivity from skull, (iii) defluorination of ^{18}F-FCWAY may be greatly prevented by miconazole in vitro and in vivo, probably through the inhibition of cytochrome P450 enzymes, and (iv) after pretreatment of rats with miconazole, ^{18}F-FCWAY is effective for imaging 5-HT_{1A} receptors in rat brain with PET because of greatly reduced radioactivity spillover from skull to adjacent brain regions; therefore, image quality is greatly enhanced. We conclude that ^{18}F-FCWAY in miconazole-treated rats may serve as an effective platform for investigating 5-HT_{1A} receptors in rat models of neuropsychiatric conditions or drug action. Moreover, this study suggests that successful inhibition of ^{18}F-FCWAY defluorination in human subjects in vivo would improve sensitivity of quantification of 5-HT_{1A} receptors in cortical regions and render ^{18}F-FCWAY even more useful for imaging of 5-HT_{1A} receptors in neuropsychiatry.

ACKNOWLEDGMENTS

We gratefully acknowledge CyDex, Inc. (Lenexa, KS) for providing Captisol; Cyrill Burger, PhD, for providing

PMOD computer software; and the Clinical Center (NIH) for providing ^{18}F-FCWAY. We are very thankful to Bik-Kee Vuong, BS; Lucka Martiniova, MS; Julie A. McCarron, PhD; Jae Seung Kim, MD; Kendra Modell, MS; Lisa Nichols, MS; Nicholas Seneca, MS; Soon-Duk Park, BS; H. Umesha Shetty, PhD; and Vanessa Cropley, MS, for useful input. This research was supported by the Intramural Research Program of the NIH/NIMH.

REFERENCES

1. Phelps ME, Mazziotta JC, Schelbert HR. *Positron Emission Tomography and Autoradiography, Principles and Applications for the Brain and Heart.* New York, NY: Raven Press; 1986.
2. Jones T. The imaging science of positron emission tomography. *Eur J Nucl Med.* 1996;23:807–813.
3. Jones T. The role of positron emission tomography within the spectrum of medical imaging. *Eur J Nucl Med.* 1996;23:207–211.
4. Fowler JS, Wolf AP. Working against time: rapid radiotracer synthesis and imaging the human brain. *Acc Chem Res.* 1997;30:181–188.
5. Halldin C, Gulyas B, Langer O, et al. Brain radioligands: state of the art and new trends. *Q J Nucl Med.* 2001;45:139–152.
6. Elsinga PH. Radiopharmaceutical chemistry for positron emission tomography. *Methods.* 2002;27:208–217.
7. Sedvall G. PET scanning as a tool in clinical psychopharmacology. *Triangle.* 1991;30:11–12.
8. Burns HD, Hamill TG, Eng W, et al. Positron emission tomography neuroreceptor imaging as a tool in drug discovery, research and development. *Curr Opin Chem Biol.* 1999;3:388–394.
9. Comar D, ed. *PET for Drug Development and Evaluation.* Boston, MA: Kluwer Academic Publishers; 1995.
10. Farde L. The advantage of using positron emission tomography in drug research. *Trends Neurosci.* 1996;19:211–214.
11. Lang L, Jagoda E, Schmall B, et al. Development of fluorine-18-labeled 5-HT$_{1A}$ antagonists. *J Med Chem.* 1999;42:1576–1586.
12. Drevets WC, Frank E, Price JC, et al. PET imaging of serotonin 1A receptor binding in depression. *Biol Psychiatry.* 1999;46:1375–1387.
13. Toczek MT, Carson RE, Lang L, et al. PET imaging of 5-HT$_{1A}$ receptor binding in patients with temporal lobe epilepsy. *Neurology.* 2003;60:749–756.
14. Carson RE, Lang L, Spanaki M, et al. Human 5-HT$_{1A}$ PET studies with [^{18}F]FCWAY [abstract]. *Neuroimage.* 2000;11(suppl):S45.
15. Kharasch ED, Thummel KE. Identification of cytochrome P450 2E1 as the predominant enzyme catalyzing human liver microsomal defluorination of sevoflurane, isoflurane, and methoxyflurane. *Anesthesiology.* 1993;79:795–807.
16. Yin H, Anders MW, Jones JP. Metabolism of 1,2-dichloro-1-fluoroethane and 1-fluoro-1,2,2-trichloroethane: electronic factors govern the regioselectivity of cytochrome P450-dependent oxidation. *Chem Res Toxicol.* 1996;9:50–57.
17. Seidel J, Vaquero JJ, Green MV. Resolution uniformity and sensitivity of the NIH ATLAS small animal PET scanner: comparison to simulated LSO scanners without depth-of-interaction capability. *IEEE Trans Nucl Sci.* 2003;50:1347–1350.
18. Johnson CA, Seidel J, Vaquero JJ, et al. Exact positioning for OSEM reconstructions on the ATLAS depth-of-interaction small animal scanner [abstract]. *Mol Imaging Biol.* 2002;4(suppl):S22.
19. Liow JS, Johnson CA, Toyama H, et al. A single slice rebinning/2D exact positioning OSEM reconstruction for the NIH ATLAS small animal PET scanner [abstract]. *J Nucl Med.* 2003;44(suppl):163P.
20. George P, Watson C. *The Rat Brain in Stereotaxic Coordinates.* 4th ed. San Diego, CA: Academic Press; 1998.
21. Piel G, Evrard B, Van Hees T, et al. Comparison of the IV pharmacokinetics in sheep of miconazole-cyclodextrin solutions and a micellar solution. *Int J Pharm.* 1999;180:41–45.
22. Fujimaki Y, Arai N, Inaba T. Identification of cytochromes P450 involved in human liver microsomal metabolism of ecabapide, a prokinetic agent. *Xenobiotica.* 1999;29:1273–1282.
23. Martinez C, Albet C, Agundez JA, et al. Comparative in vitro and in vivo inhibition of cytochrome P450 CYP1A2, CYP2D6, and CYP3A by H_2-receptor antagonists. *Clin Pharmacol Ther.* 1999;65:369–376.
24. Rendic S. Drug interactions of H_2-receptor antagonists involving cytochrome P450 (CYPs) enzymes: from the laboratory to the clinic. *Croat Med J.* 1999;40:357–367.
25. Zweers-Zeilmaker WM, Horbach GJ, Witkamp RF. Differential inhibitory effects of phenytoin, diclofenac, phenylbutazone and a series of sulfonamides on hepatic cytochrome P4502C activity in vitro, and correlation with some molecular descriptors in the dwarf goat (Caprus hircus aegagrus). *Xenobiotica.* 1997;27:769–780.
26. Tassaneeyakul W, Birkett DJ, Miners JO. Inhibition of human hepatic cytochrome P4502E1 by azole antifungals, CNS-active drugs and non-steroidal anti-inflammatory agents. *Xenobiotica.* 1998;28:293–301.
27. Maurice M, Pichard L, Daujat M, et al. Effects of imidazole derivatives on cytochromes P450 from human hepatocytes in primary culture. *FASEB J.* 1992;6:752–758.
28. Denner K, Vogel R, Schmalix W, et al. Cloning and stable expression of the human mitochondrial cytochrome P45011B1 cDNA in V79 Chinese hamster cells and their application for testing of potential inhibitors. *Pharmacogenetics.* 1995;5:89–96.
29. Chang TK, Gonzalez FJ, Waxman DJ. Evaluation of triacetyloleandomycin, alpha-naphthoflavone and diethyldithiocarbamate as selective chemical probes for inhibition of human cytochromes P450. *Arch Biochem Biophys.* 1994;311:437–442.
30. Graybill JR, Craven PC. Antifungal agents used in systemic mycoses: activity and therapeutic use. *Drugs.* 1983;25:41–62.
31. Heel RC, Brogden RN, Pakes GE, et al. Miconazole: a preliminary review of its therapeutic efficacy in systemic fungal infections. *Drugs.* 1980;19:7–30.
32. Carson RE, Lang L, Watabe H, et al. PET evaluation of [^{18}F]FCWAY, an analog of the 5-HT$_{1A}$ receptor antagonist, WAY-100635. *Nucl Med Biol.* 2000;27:493–497.
33. Hume SP, Ashworth S, Opacka-Juffry J, et al. Evaluation of [*O-methyl*-^{3}H]WAY-100635 as an in vivo radioligand for 5-HT$_{1A}$ receptors in rat brain. *Eur J Pharmacol.* 1994;271:515–523.
34. Hume SP, Gunn RN, Jones T. Pharmacological constraints associated with positron emission tomographic scanning of small laboratory animals. *Eur J Nucl Med.* 1998;25:173–176.